Journal of Advanced Research 24 (2020) 211–222

Contents lists available at ScienceDirect

Journal of Advanced Research

journal homepage: www.elsevier.com/locate/jare

Robustness of anaerobes exposed to cyanuric acid contaminated wastewater and achieving efficient removal via optimized co-digestion scheme

Kabir Abdullahi [a], Ahmed Elreedy [b,c,*], Manabu Fujii [b], Mona G. Ibrahim [a,d], Ahmed Tawfik [e]

[a] Environmental Engineering Department, Egypt-Japan University of Science and Technology, Alexandria 21934, Egypt
[b] Department of Civil and Environmental Engineering, Tokyo Institute of Technology, Meguro-ku, Tokyo 152-8552, Japan
[c] Sanitary Engineering Department, Alexandria University, Alexandria 21544, Egypt
[d] Environmental Health Department, High Institute of Public Health, Alexandria University, Alexandria 21544, Egypt
[e] Water Pollution Research Department, National Research Centre, Giza 12622, Egypt

GRAPHICAL ABSTRACT

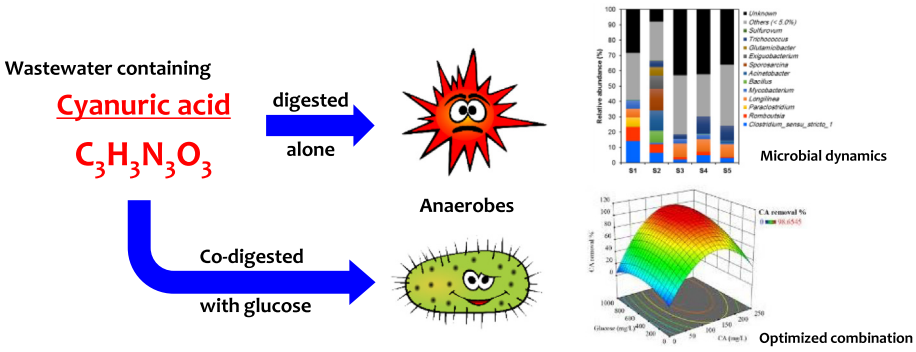

ARTICLE INFO

Article history:
Received 10 September 2019
Revised 7 February 2020
Accepted 11 February 2020
Available online 17 February 2020

Keywords:
Cyanuric acid
Anaerobic treatment
Industrial wastewater
Co-digestion
Microbial dynamics

ABSTRACT

The impact of various industrial pollutants on anaerobes and the biodegradation potentials need much emphasis. This study aims to investigate the response of anaerobic microbial systems to cyanuric acid (CA) exposure; CA is toxic and possible carcinogen. First, the long-term exposure of mixed culture bacteria (i.e., municipal sludge) to low-strength wastewater containing 20 mg/L CA was conducted in an up-flow anaerobic staged reactor. Stable performance and sludge granulation were observed, and the microbial community structure showed the progression of genus *Acinetobacter* known as CA degrader. Second, batch-mode experiment was performed to examine the CA biodegradability at higher doses (up to 250 mg/L of CA) in the absence and presence of glucose as a co-substrate; response surface-based optimization was used to design this experiment and to estimate the optimum CA-glucose combination. CA removal of 77–98% was achieved when CA was co-digested with glucose (250–1,000 mg/L), after 7 days-incubation at temperature of 37 °C, compared to 34% when CA was solely digested. Further, the obtained methane yield dropped when CA exceeded over 125 mg/L, though the deterioration was mitigated by addition of higher concentration of glucose. Overall, we conclude that CA is efficiently degraded under anaerobic conditions when being co-digested with readily assimilable substrate.

Peer review under responsibility of Cairo University.
* Corresponding author at: Department of Civil and Environmental Engineering, Tokyo Institute of Technology, Meguro-ku, Tokyo 152-8552, Japan.
E-mail addresses: elreedy.a.aa@m.titech.ac.jp, ahm_nazem@alexu.edu.eg (A. Elreedy).

https://doi.org/10.1016/j.jare.2020.02.006
2090-1232/

Introduction

Cyanuric acid (2,4,6-Trihydroxy-1,3,5-triazine; $C_3H_3N_3O_3$; CA) is a trifunctional s-triazine compound adopting the heterocyclic triazine skeleton. Although it was reported to be a natural product, the occurrence of this compound in natural environments may be attributed to a combination of anthropogenic activities, such as industrial synthesis, abiotic processes, and microbial synthesis [1]. CA is toxic and causes behavioral deviation (e.g., difficulty in mating or finding food) for aquatic organisms such as zooplankton, fishes, and larval lampreys [2]. For humans, CA is reported to exhibit low toxicity, but this compound is a possible carcinogen or a suspected gastrointestinal toxicant when ingested together with melamine [3]. The long-term effect of CA on aquatic ecosystem remains unknown; thus this compound is included in the European commission (EC) list for environmental priority pollutants [2,4]. Since its first introduction, CA has become an industrially important compound which is continually synthesized and used as a precursor in the manufacture of complexes and cross-linked polymers such as pesticides, herbicides, disinfectants, resins, and pigment production for textile industry [1,3,5]. CA has been also applied in swimming pools as a disinfectant stabilizer [6]. The large quantity of CA production, its intensive use, and its inherent chemical stability resulted in the accumulation and contamination of water and soil environments. Indeed, CA has been repeatedly detected in drinking water at concentrations above the limit set by World Health Organization (WHO) (40 mg/L CA).

Because of its stability, CA has generally shown recalcitrant properties to the chemical and biological degradation processes. CA removal during the industrial wastewater treatment as well as the environmental degradation processes involves either abiotic processes such as chemical and photochemical reactions [7,8] or biotic transformations mediated by microorganisms [9]. Several studies for the removal of s-triazine compounds have been carried out by chemical or photochemical method [2], soil-charcoal perfusion method [10] and bacterial encapsulation [3]. Advanced oxidation processes (AOPs) have shown high degradation efficiency dealing with various pollutants [11–13]; however, its capital and running costs has made it a less sustainable option particularly in the developing countries. Each of these methods have its own disadvantage and limitations. In contrast, bioremediation using microbes is found to be effective and most inexpensive process that is recognized for degrading organic pollutants, e.g., s-triazine family [14].

Aquatic microbes capable of metabolizing CA is anticipated to be widespread in a range of environments, with degradation genes being detected in Egypt, India, China, Brazil, USA, Canada, France, and many other parts of the world with over 97% similarities [15–17]. Successful reports mostly using pure culture bacteria have shown that CA can be biologically degradable, and few microbial species possess metabolic capability to biodegrade CA [18]. Experimentally, it was reported that 1 mol of CA is stoichiometrically converted into 2 mol each of ammonia and carbon dioxide in hydrolytic pathway mediated by three enzymes (i.e., CA hydrolase [CAH]; biuret hydrolase [BH], and allophanate hydrolase [AH]); CAH hydrolytically cleaves the s-triazine ring to produce biuret; subsequently, BH enzymatically hydrolyzes biuret to produce allophanate with the release of ammonia; finally, allophanate is hydrolyzed by AH forming 2 mol of ammonia and carbon dioxide [1,19].

Indigenous mixed cultures can be an alternative option for the successful bioremediation of pollutants, since xenobiotic compounds are degraded by the mixed microbial communities mostly found in natural environment. Further, the anaerobic digestion process has been successfully used to treat a range of pollutants as environmentally-friendly approach [20–26]. The co-digestion scheme with readily biodegradable organics has also been employed in the treatment of slowly biodegradable organics, such as the lignocellulosic wastes [27], yielding a high efficiency. Therefore, we investigated the biodegradation of CA by anaerobic co-digestion scheme using mixed culture microbes. More specifically, this study aimed firstly to assess the development of inoculum (municipal sludge) and associated microbial composition, and performance during the long-term operation of an up-flow anaerobic staged reactor (UASR) being supplemented with low-strength wastewater (0.6 gCOD/L/d) containing 20 mgCA/L. The second objective was to optimize a co-digestion scheme with different glucose concentrations (up to 1000 mg/L) via response surface method (RSM), in order to assess the CA biodegradation efficiency under high CA contamination level (up to 250 mg/L). The findings obtained in this work could provide useful insights into the impact of this potential carcinogen on the biological treatment processes, and the ability of microbial mixed culture to degrade CA at varied concentrations found in both domestic sewer systems and industrial effluents.

Materials and methods

Inoculum and UASR continuous operation

The inoculum sludge used in this study was collected from a municipal wastewater treatment plant, Alexandria, and then was feed under anaerobic conditions. The initial average concentrations of total solids (TS) and volatile solids (VS) for the collected sludge were 88 and 41 g/L, respectively, resulting in VS/TS ratio of 0.46. CA with a purity of 98% was employed. The synthetic feed composition (in mg/L) including nutrients and CA was 31 for KH_2PO_4, 300 for $MgSO_4{\cdot}7H_2O$, 10 for NaCl, 10 for $CaCl_2{\cdot}2H_2O$, 165 for $(NH_4)_2SO_4$, 20 for CA and 280 for glucose. Trace metals solution was also added to the feed with its final concentrations (in mg/L) were, as reported by An et al. [4], 10 for EDTA, 0.12 for $ZnSO_4{\cdot}7H_2O$, 0.03 for $CuSO_4{\cdot}5H_2O$, 0.12 for $MnCl_2{\cdot}4H_2O$, 0.18 for KI, 0.15 for $CoCl_2{\cdot}6H_2O$, 0.15 for H_3BO_4, 0.06 for $Na_2MoO_4{\cdot}2H_2O$, 1.5 for $FeCl_3{\cdot}6H_2O$ The initial pH of the feed was kept at ~7.2 and pH adjustment was not performed as pH of the feed (i.e., influent) was relatively stable during the operation.

UASR of 42 L working volume, consisting of four upward compartments (Fig. 1), was used for feeding and acclimatizing the collected inoculum during the period of 104 d. 16 L of sludge, representing ~38% of the reactor working volume, was inoculated. Given the equivalent chemical oxygen demand (COD) (due to the addition of glucose and CA) and applied hydraulic retention time (HRT) of 12 h, organic loading rate (OLR) of 0.6 gCOD-glucose/L/d, containing 0.04 gCOD-CA/L/d, was employed. During the operation of UASR at ambient temperature (18–28 °C), the COD, NH_4^+-N, and pH profiles, sludge characteristics, and microbial community dynamics were monitored to highlight the long-term impact of CA contamination. A relatively low concentration of 20 mg/L was employed during the long-term continuous system. Eventually, such operational conditions, particularly ambient temperature, were employed to provide implications for studying the potential contamination of sewer systems by CA (where temperature generally varies).

Batch-mode experiment and optimization approach

Prior to the batch-type experiment, seed sludge, collected from UASR (VS/TS ratio reached 0.66), was further acclimatized for 14 days using a batch-feed substrate composed of glucose (1,000 mg/L) and CA (100 mg/L) at higher concentrations compared

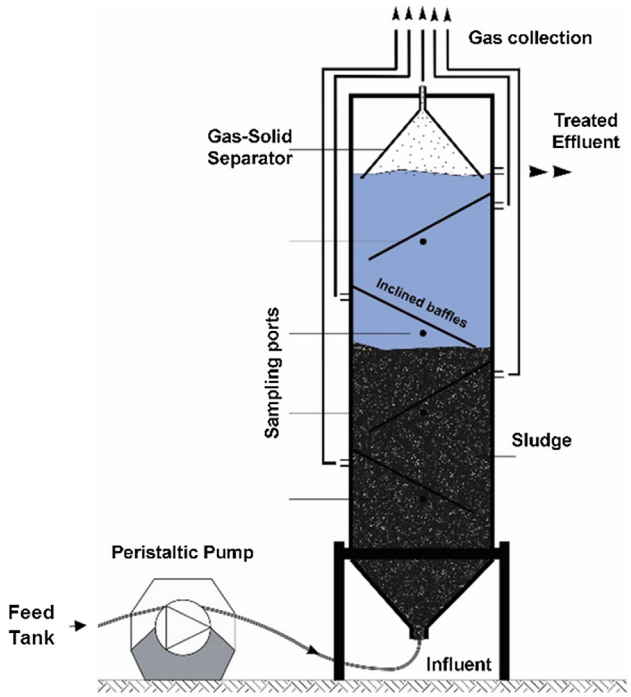

Fig. 1. Schematic diagram of up-flow anaerobic staged reactor (UASR) used in this study.

to the continuous system. The experiment was performed using serum bottles with a working volume of 500 mL and headspace of 50 mL. 250 mL aliquots of the acclimatized sludge were added into the serum bottles, resulting in mixed liquor of 13.4 gVS/L. The COD:N:P, in each bottle, was adjusted according to the ratio of 400:7:1, using NH_4Cl and KH_2PO_4 [28,29]. Initial pH, for all batches, were adjusted to 7.0, using NaOH or HCl. The batch cultures were then incubated at a temperature of 37 °C and shacked regularly. Duplicate runs were performed, and average ± standard deviation of results was calculated.

The experimental design was determined using RSM and two-factors central composite design (CCD), via Design Expert 11 software. Two independent variables, i.e., CA (with range from 0 to 250 mg/L) and glucose (0–1,000 mg/L) were selected to be optimized variables, and the resulted combinations are shown in Table 1. In this analysis, the fitting surfaces for different responses (e.g., methane production, CA, and COD removals) and associated independent variables are produced according to the quadratic model (Eq. (1)), as noted below.

$$Y = A_0 + A_1X_1 + A_2X_2 + A_{12}X_1X_2 + A_{11}{X_1}^2 + A_{22}{X_2}^2, \quad (1)$$

where Y is the different responses, X_1 is the initial CA, X_2 is the initial glucose, A_0 is the model constant, and A_i and A_{ii} are the model predicted linear coefficients. Moreover, the RSM technique estimates the optimum conditions, within the designed ranges, via interpolation using second order polynomial regression.

Analytical methods

Analysis for total ammonia-nitrogen (as NH_4^+-N), TS, VS and total volatile fatty acids (TVFA) were carried out according to the standard method by American Public Health Association [30]. COD concentrations were analyzed using HACH DR/3900 spectrophotometer according to the standard methods [31]. Further, the total biogas volume was measured by water displacement method, and then the gas composition was quantified using gas chromatography (GC-2014, Shimadzu, Japan) [32]. CA concentration was determined using liquid chromatography-mass spectrometry (LCMS-2020, Shimadzu) with an APCI interface on negative polarity. The measurement conditions are as follows; i.e., shimpack XR-ODS II column with a size of 3 × 100 mm was used; the mobile phase was 90% acetonitrile and 10% of 0.1 formic acid solution at a flow rate of 0.4 mL/min; the oven temperature was 30 °C, and the retention time was 5 min.

Scanning electron microscopy (SEM) analysis for sludge samples was performed to examine the surface morphology change after long-term exposure to CA (Hitachi S-4500, Japan). Sludge samples were fixed in a 0.2 M phosphate buffer containing 6% glutaraldehyde for 1 h at 4 °C. After fixation, samples were washed three times in 0.1 M phosphate buffer for 2 h. Samples were then dehydrated gradually in a series of ethanol solutions (i.e., 50, 70, 95, 100, and then 100%). Drying was achieved via overnight incubation at 30 °C. Samples were then coated and analyzed as previously described by Ismail and Tawfik [33]. X-ray diffraction (XRD) analysis was performed using a Shimadzu XRD-6100 with a Cu anode, operated at 30 mA and 40 kV using divergence, scatter and reception slits of 1, 1, and 0.3 mm, respectively. The XRD profiles were measured in a scan range of 5–80° and a scan speed of 12 deg/min. Fourier Transform Infra-Red (FTIR) analysis was also performed using a spectrometer covering a wavenumber range of 400–4,000 cm^{-1} (Shimadzu IR Prestige-21; Bruker spectrometer model). The spectra were obtained at a resolution of 4 cm^{-1}.

Microbial analysis

Sludge samples were collected from the bottom of UASR on day 0 (S1), day 22 (S2), day 53 (after the 1st steady state; S3), and day 95 (after reaching the last steady state; S4 [from the reactor bottom] and S5 [from the 2nd upward compartment]) were collected on day 95 to examine the variation along the reactor length. The 16S rRNA gene region was targeted using next generation sequencing (NGS). The primers 341F: 5′-CCTACGGGNGGCWGCAG-3′ and 805R: 5′-GACTACHVGGGTATCTAATCC-3′, for the V3 and V4 regions, were used to identify the bacterial community affected by CA exposure [34,35]. The procedures related to DNA extraction, polymerase chain reaction (PCR), and repeated purifications were carried out based on the manufacturer protocols and as previously described by Ali et al. [36]. The major equipment and kits used in such procedures are as follows; DNeasy PowerSoil kit (REF. 12888-50, Qiagen) for DNA extraction, Agencourt AMpure XP PCR beads solution (Beckman Coulter) for purifications, NanoDrop 2000 spectrophotometer (Thermo Fisher Scientific), TaKaRa PCR Thermal Cycler Dice (Takara Bio), Agilent 2100 bioanalyzer, and DNA 1000 Kit (No. 5067-1505, Agilent). Then, for gene sequencing, Illumina MiSeq 2500 was conducted at Hokkaido System Science Co. (Sap-

Table 1
Experimental parameters determined from the response surface analysis using two-factors central composite design (CCD); i.e., X_1 for cyanuric acid (CA) and X_2 for glucose.

Run	1	2	3	4	5	6	7	8	9
X_1 (CA)	125	125	0	125	0	250	62.5	250	187.5
X_2 (Glucose)	500	250	1,000	750	0	1,000	500	0	500

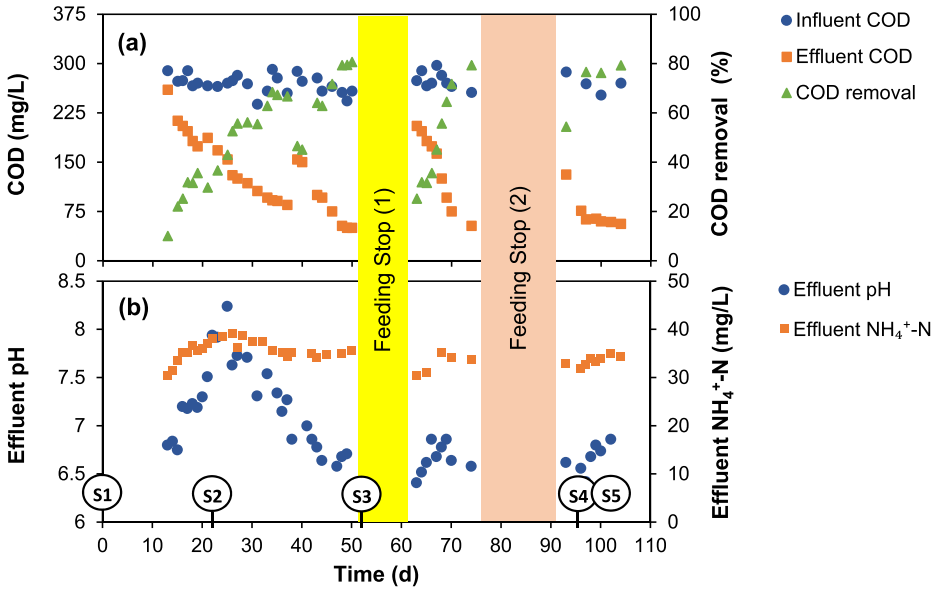

Fig. 2. Performance of up-flow anaerobic staged reactor (UASR) when cyanuric acid (CA) contaminated low-strength wastewater was fed as substrate: variations of COD concentrations and removal efficiency (a), and NH_4^+-N and pH (b). The feeding was stopped between first and second phases (Feeding Stop (1)) and between second and third phases (Feeding Stop (2)). Symbols S1-S5 refer to the collected sludge samples for microbial analysis.

poro, Japan); the raw reads were then processed using R software (version 3.4.3), and based on Silva database (ver. 128). Further, principal components analysis (PCA), using Minitab 18 software, was conducted to emphasize the microbial dynamics between different samples' bacterial composition (at genus level).

Results and discussion

Long term exposure to CA (20 mg/L) contaminated low-strength wastewater

Overall efficiency

The long-term impact of CA on anaerobes was studied in an UASR for a period of 105 days. Fixed OLR (0.6 gCOD/L/d and 0.04 gCA/L/d) and HRT (12 h) were used throughout the experiment with two operational stops (the feeding pump was stopped during these two periods), as shown in Fig. 2. The overall efficiency of the system was assessed by the COD, NH_4^+-N and pH responses. The COD removal efficiency gradually increased from 10 to 80%, by reaching the first steady state (Fig. 2a). The slow start-up indicated that CA contamination caused a relatively long adaptation period (i.e., 50 days). During the second and third phases of operation, the COD removal reached a comparable value ~80% within shorter period, emphasizing the induced performance stability when CA up to 20 mg/L was existed with 280 mg-glucose/L at ambient temperature.

Further, Fig. 2b shows a steady increase in NH_4^+-N concentration, in the first operational phase, resulting in net NH_4^+-N release of ~6.4 mg/L. The steady NH_4^+-N release observed in the medium could be due to the biodegradation of CA. The anaerobic biodegradation of CA can proceed as described in Eq. (2), which theoretically yields 6.5 mgN/L at 20 mgCA/L. Hence, catabolic degradation of CA into NH_4^+-N can be considered as the major source of NH_4^+-N steady release. Similar steady releases on NH_4^+-N were observed in the remaining two operational phases (after the two feeding-stops). Fig. 2b also shows the effluent pH variation, as the influent pH was maintained in the range of 7.0–7.5. The steady effluent pH varied from 6.6 to 6.9 during the three operational phases; however, a peak value of pH 8.2 corresponded with maximum NH_4^+-N release was observed. The increased NH_4^+-N observed before reaching the first steady state is mainly attributed to the ammonification of protein derived from dead cells.***

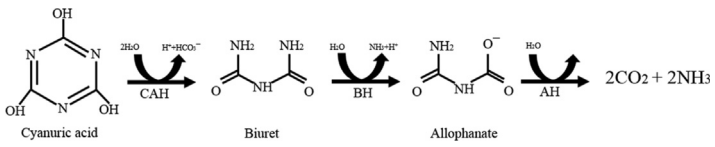

(2)

Microbial community structure

Next generation sequencing analysis was applied to microbial samples taken from UASR bottom on day 0 (S1), day 22 (S2), day 58 (S3) and day 95 (S4 from the bottom and S5 from the 2nd upward compartment). Net detected reads were assigned to 6,958 operational taxonomic units (OTUs), at a similarity level of 97%. The dominant phyla observed within the microbial population over the duration of experiment, as shown in Fig. 3, were *Firmicutes* (9.7–58.8%), *Chloroflexi* (2.7–26.8%), *Proteobacteria* (7.3–39.0%), *Actinobacteria* (1.4–14.2%), *Planctomycetes* (2.3–13.7%), *Bacteroidetes* (1.9–25.2%), *Caldiserica* (0.1–4.6%) and *Spirochaetae* (0.0–2.6%).

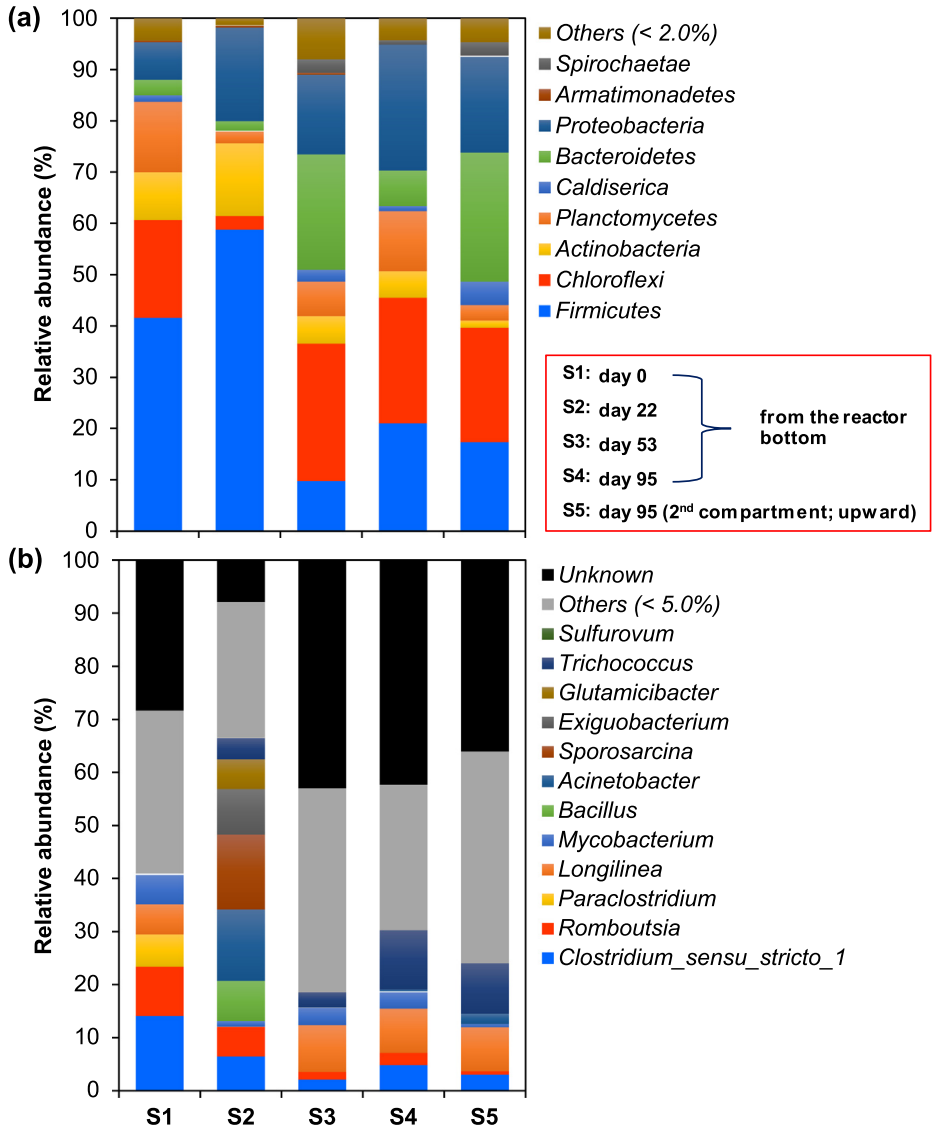

Fig. 3. Bacterial relative abundance for sludge samples collected at different time intervals when CA-contaminated low-strength wastewater was used as substrate, at phylum level (a), and genus level (b).

Comparing three samples (S2, S3, and S4) indicates that the substantial difference from others was observed for S2 where transitional state was recorded for effluent water quality (e.g., higher NH_4^+-N release and lower COD removal in Fig. 2). This observation also suggests the necessity of relatively long period (e.g., ~50 d) for microbial adaptation (e.g., the granules formation, CA degradation as well as the polishing of dead cells potentially present in initial sludge) to the imposed conditions. The notable increase in relative abundance of *Actinobacteria* (from ~5 to ~14%), in S2, whose members are known to be able to decompose the organics derived from dead microbes, supports this hypothesis [37]. In addition, phylum *Spirochaetae* gradually appeared in S2-S4 (up to relative abundance of 2.6%), which was reported to participate in fermentation of carbohydrates (e.g., glucose) into acetate, H_2 and CO_2 [38]. Members from phylum *Spirochaetae* (belonging to family *Spirochaetaceae*; > 93%) form a helically coiled shape, which is likely consistent with the SEM image of sludge after treatment (as shown later in Fig. 5b). On the other hand, variations in abundance of some phyla (i.e., *Firmicutes*, *Bacteroidetes*, and *Proteobacteria*) were found among samples collected from the 1st (S3) and last (S4) steady states.

Likewise, the genus level classification showed higher diversity and different genera in S2 (i.e., 14.1% for *Sporosarcina*, 8.6% for *Exiguobacterium*, and 5.6% for *Glutamicibacter*) as compared to S3-S5. Among samples of S3-S5, the dominant genera were *Acinetobacter* (0.0–13.4%), *Trichococcus* (2.9–11.2%), *Clostridium_sensu_stricto_1* (2.1–7.9%), *Longilinea* (0.1–8.8%), *Romboutsia* (0.6–5.6%), and *Mycobacterium* (0.6–3.3%). Particularly, it was noticed that the abundance of *Acinetobacter* and *Trichococcus* were highly associated with samples collected during the continuous feeding of glucose and CA based substrate (i.e., S2, S4, and S5; note that continuous feeding was not the case for S1 and S3). Genus *Acinetobacter* was previously reported to possess the ability to degrade CA [2], as well as other triazine compounds (e.g., atrazine and cyanazine) [39]. Moreover, genus *Trichococcus*, which was previously found in sewage, had an ability to grow at in a wide range of temperatures from 4 to 39 °C and showed a positive correlation with *Acinetobacter* abundance [40,41]. The progressed abundance

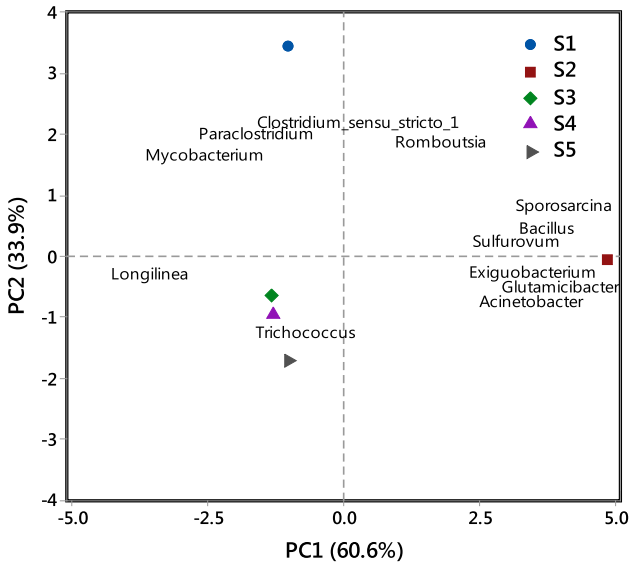

Fig. 4. Principal component analysis (PCA) related score plot considering the bacterial abundance at genus level and different time intervals (S1 for day 0, S2 for day 22, S3 for day 53, S4 [bottom of UASR] and S5 [2nd compartment, upward] for day 95).

of *Trichococcus* could be attributed to its preferable growth at high urea-containing medium [40] and higher ammonia-tolerance [42], given that urea can be the main intermediate by-product during the anaerobic biodegradation of CA.

Moreover, to demonstrate the microbial community variation along the UASR height, results of samples S4 were compared to S5 at phylum level, showing decrements in fermentation-related phyla (i.e., *Actinobacteria* and *Firmicutes*) along with increments in other phyla such as *Bacteroidetes* and *Caldiserica*. While members of phylum *Bacteroidetes* are recognized to be able to utilize a wide range of substrates, including urea, and higher ammonia-tolerance [43], members from phylum *Caldiserica* are known to be sulfur-oxidizing anaerobic bacteria [44]. The finding that abundance of the potential CA degrader genus, i.e., *Acinetobacter*, increased from 0.3% (S4) to 1.9% (S5) (Fig. 3b) emphasizes the higher biodegradability of CA can be achieved by employing longer HRT as well as the longer path length UASR. Furthermore, the PCA results in Fig. 4 show that 1st and 2nd components (i.e., PC1 and PC2) together achieved 94.5% of the variance. The PCA score plot in Fig. 4 demonstrates that: (1) the substantial change along the operation period (S1, S2 and S3), (2) the UASR performance showed stability after the two feeding-stops (S3 and S4), and (3) the UASR configuration, considering the multiple upward compartments,

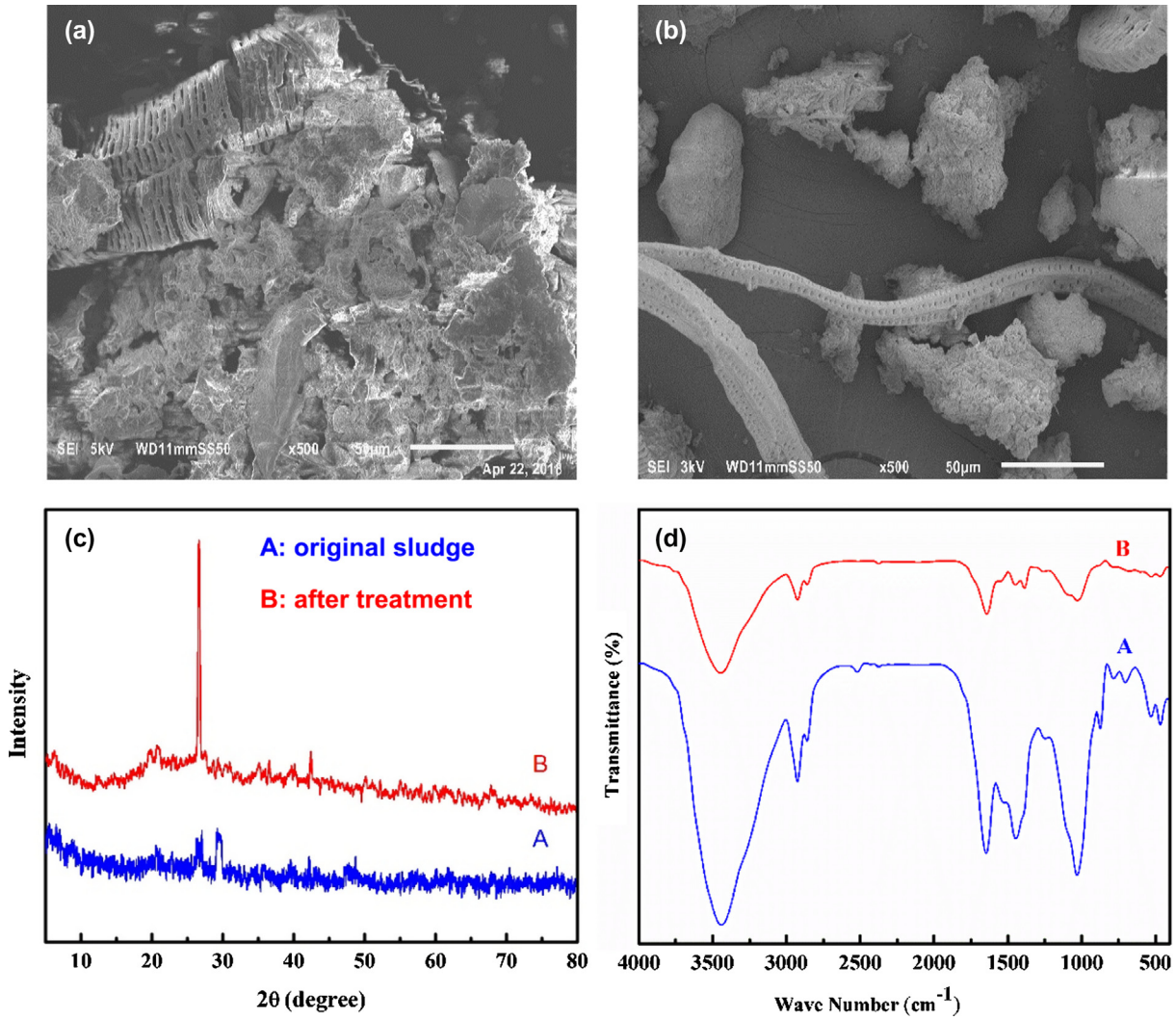

Fig. 5. Sludge characteristics before and after the long-term exposure to wastewater containing cyanuric acid: SEM image for original sludge (a) and SEM image for sludge after the treatment (b), XRD spectra for samples before and after treatments (c), and FTIR spectra for samples before and after treatments (d).

provided an ability to change the microbial composition along the reactor length (S4 and S5).

Sludge characteristics before and after treatment

The SEM, XRD, and FTIR analyses of the inoculum sludge were carried out for the initial and after 45 days of treating CA-contaminated wastewater, in order to examine the characteristic changes in the sludge properties. Fig. 5a and 5b show the SEM images of sludge before and after treatment, respectively. Before the treatment, heterogeneous structure and roughness as well as the presence of thinly spiraled shape microorganisms were observed. After the treatment, the sludge morphology indicated stable granulation and presence of helically coiled bacterial cells which are likely related to *Spirochetes*-like members. Moreover, Fig. 5c shows the XRD pattern of the sludge; before the treatment, the XRD pattern exhibited some broad peaks of the amorphous halo and some sharp peaks of crystalline components at 26.3, 27.0 and 29.2°, representing quartz, calcite, and kaolinite, respectively [45,46]. After the treatment, disappearance of calcite and kaolinite peaks, and rapid increase of quartz peak (at 26.3°) were observed (Fig. 5c); the formation of quartz could be associated with kaolinite when being partially hydrolyzed [47]. Moreover, the crystallinity index of the sludge was 85.5% (before treatment), and then decreased to 57.8% (after treatment). These observations indicate that most of the crystalline polymers have been eliminated, suggesting the progressed microbial activity within the inoculum.

FTIR spectra of the sludge before and after the treatment are shown in Fig. 5d and, as noted below, obtained spectra were dis-

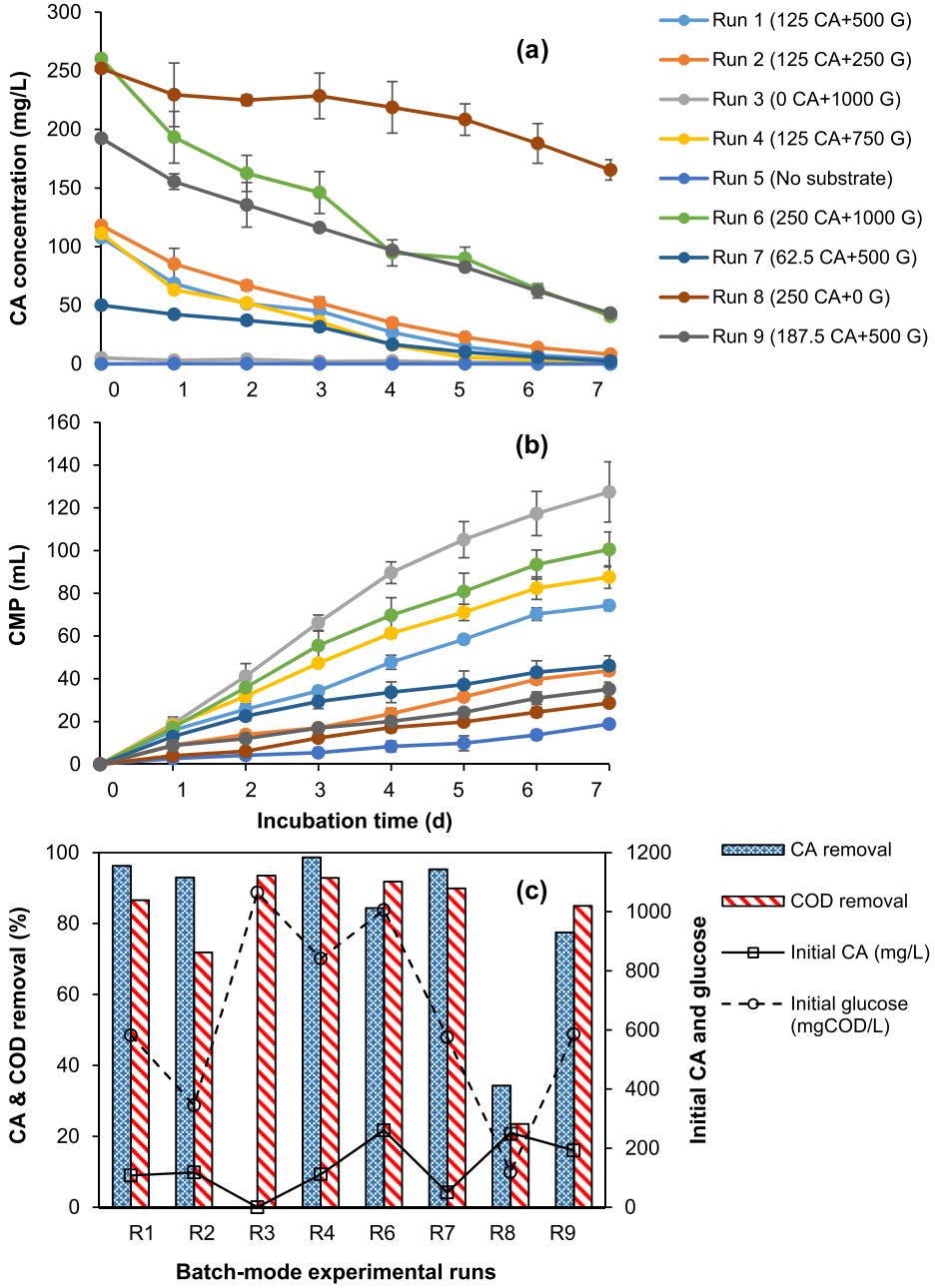

Fig. 6. Time course of anaerobic biodegradation of cyanuric acid (CA) (a) and cumulative methane production (CMP) (b), as well as the final removal efficiencies of cyanuric acid (CA) and COD (c) from the batch-mode incubation of CA and glucose at different concentrations. The co-digestion of CA and glucose (G) was employed at different concentrations (Run 1 to 9).

cussed according to the literature [48–51]. Before treatment, the most important functional groups observed were O—H and N—H groups, representing the presence of amines and amides at 3,440 cm^{-1}. Peaks at 1,650^{-1} and 450 cm^{-1} represent the C=O group for amides, ketone and peptic bond of protein. The strong peak observed at 1,030 cm^{-1} represents the stretching vibration of C—O functional group of non-structural carbohydrates. Thus, the results show the presence of bacterial constituent of carbohydrate, lipids, protein, and aromatic functional groups in the inoculum. Then, after treatment, a new band appeared at 2,375 cm^{-1}, indicating the presence of C=C stretch of protein origin; as well, another band appeared at 1,387 cm^{-1}, which is likely associated with C—N groups of primary amides II that are mainly involved in formation of protein structure. The small shoulder found at 1,545 cm^{-1} can be attributed to the C=O vibration of primary amides (a protein-derived band found in nitrogen-rich compost), as reported by De Oliveira Silva et al. [52]. Further, the decrease in intensity observed for the band at 1,030 cm^{-1} indicates the progress of the decomposition process. Overall, the sludge sample collected after treatment (day 45) was enriched in protein-like group, suggesting the stably developed microbes and associated enzymatic activities, e.g., CA hydrolase.

Assessment of CA biodegradability via co-digestion with glucose

The nine batch experimental runs were monitored for 7 consecutive days to assess the biodegradation of CA, as shown in Fig. 6. In run 1, 125 mg/L of CA and 500 mg/L of glucose were co-digested, and CA removal of 96% was achieved. In run 4 that was fed with similar CA of 125 g/L and higher glucose of 750 mg/L, CA was almost entirely used up resulting the highest CA removal of 98%. At CA up to 125 mg/L and glucose of 250–750 mg/L, the three runs (i.e., run 2, run 3, and run 4) showed a comparable degradation trend (Fig. 6a). Despite the glucose addition at highest dose (1000 mg/L) in run 6, lower CA removal of 84% was achieved as compared to runs 2–4, which is most likely as a result of the higher CA concentration causing microbial inhibition. Further, the impact of glucose co-digestion was emphasized among run 6 and run 8 where higher concentration of CA (250 mg/L) was employed. The absence of glucose deteriorated the biodegradation rate of CA (run 8), as compared to run 6 (Fig. 6a). 34% CA-degradation efficiency was observed over the incubation period in run 8. Due to the very low carbon to nitrogen ratio of CA, addition of external carbon source, such as glucose, is required to improve its biodegradation [2,53]. In the absence of such carbon-nitrogen balance, Cook et al. [54] found little CA mineralization, although some pure cultures have been reported to degrade CA at low concentrations [2,55,56]. In run 7 and run 9, identical glucose concentration of 500 mg/L was co-digested with CA doses of 62.5 and 187.5 mg/L resulting in CA removals of 95 and 77%, respectively (Fig. 6c). The low CA degradation efficiency could be also assisted by the potential accumulation of unidentified metabolites such as urea, as proposed by Radosevich et al. [57].

The daily COD, NH_4-N and TVFA concentrations in the batch cultures are shown in Table 2. Over 70% of the COD were consumed after 24 h of incubation in all the batches. Run 3 (no CA and 1000 mg/L glucose) showed the highest COD removal efficiency of 94% (Fig. 6c), whereas run 2 (125 mg/L CA and 250 mg/L glucose) had the least of 72%. This could be due to the relatively low glucose as compared with the added CA dose. From these results, the presence of CA inhibited the COD removal via anaerobic digestion process. As aforementioned, the increase in NH_4-N concentration can be associated with the degradation of CA. Table 2 shows that NH_4-N was generated during the first 24 h, in all batches. After the first 48 h, decrement NH_4-N release was observed, which is consistent with the previous report by Radosevich et al. [57]. The degree of NH_4^+-N release was found to decrease with increasing glucose concentration, which is also consistent with earlier study Ernst and Rehm [58]. It should be noted that the release of NH_4^+-

Table 2
Time course of COD, total volatile fatty acids (TVFA), and NH_4-N when co-digestion of cyanuric acid (CA) and glucose (G) was employed at different concentrations in batch-type incubation (Run 1 to 9).

Batches	Results	Incubation time (d)							
		0	1	2	3	4	5	6	7
Run 1	COD	583	200	131	124	115	131	115	78
	TVFA	90	113	118	109	135	157	154	126
	NH_4-N	22	43	53	64	68	71	76	78
Run 2	COD	345	153	140	123	176	212	183	97
	TVFA	91	157	135	176	154	148	150	116
	NH_4-N	17	42	57	64	68	71	74	81
Run 3	COD	1065	542	487	291	123	108	97	69
	TVFA	91	227	222	244	268	172	165	184
	NH_4-N	31	31	34	31	39	49	49	53
Run 4	COD	842	357	309	222	134	108	77	60
	TVFA	91	157	162	191	203	198	191	141
	NH_4-N	26	51	62	69	69	71	73	79
Run 5	COD	–	178	151	133	128	149	136	91
	TVFA	–	90	104	120	102	117	110	108
	NH_4-N	–	24	31	34	36	45	46	44
Run 6	COD	1006	585	510	375	186	139	110	82
	TVFA	91	183	208	174	208	176	183	186
	NH_4-N	31	52	88	107	111	114	116	116
Run 7	COD	576	257	272	165	223	75	78	58
	TVFA	91	111	94	147	150	120	130	124
	NH_4-N	22	41	40	49	56	58	60	67
Run 8	COD	119	180	152	141	153	107	92	91
	TVFA	91	92	171	154	164	150	159	127
	NH_4-N	24	43	69	73	79	91	96	108
Run 9	COD	586	230	259	204	189	179	121	88
	TVFA	91	186	200	212	174	172	130	152
	NH_4-N	22	56	52	63	69	82	85	99

Run 1: 125 CA + 500 G; Run 2: 125 CA + 250 G; Run 3: 1000 G; Run 4: 125 CA + 750 G; Run 5: no substrate; Run 6: 250 CA + 1000 G; Run 7: 62.5 CA + 500 G; Run 8: 250 CA; Run 9: 187.5 CA + 500 G.

N was found to be negligible in the control sample (i.e., run 3 where CA was not added). The uptake of CA by microbial species can be inhibited by the presence of readily consumable nitrogen sources such as ammonia, urea, and serine [59]. Hence, this could explain the lack of complete removal of CA in our systems, though the substantial release of ammonia indicates that the CA ring can be mineralized in the large extent. In addition, Table 2 shows that the level of TVFA generation was higher in the absence of CA (run 3) compared to the CA-amended culture medium at similar glucose content (run 6). This observation reveals that the presence of CA affected the bacterial metabolic pathway rather than the VFA consumption by archaea to produce methane; this could be explained by the CA-derived impact on bacterial composition in the medium.

Regarding the cumulative methane production (CMP), Fig. 6b shows that the highest CMP of 127 mL was found in the absence of CA (run 3: no CA and 1,000 mg/L glucose). In run 6 (250 mg/L CA and 1,000 mg/L glucose), slightly lower CMP (100 mL) was obtained despite of the presence of CA. In run 1 (125 mg/L CA and 500 mg/L glucose), run 7 (62.5 mg/L CA and 500 mg/L glucose) and run 9 (187.5 mg/L CA and 500 mg/L glucose) where lower glucose concentration was employed, lower CMPs of 74, 46, and 36 mL, respectively, were recorded. These observed decrease in biogas production is most likely attributed to the lower glucose availability in the system. It is also interesting to note that discernible amount of methane (29 mL of CMP) can be produced in the absence of co-substrate (i.e., glucose) as shown in the treatment of run 8 (250 mg/L CA and no glucose). Overall, the CMP was largely dependent on the initial glucose concentration, and the presence of CA showed relatively small inhibitory effect on methane production when high concentration of glucose (i.e., 1,000 mg/L) was employed.

Optimization of CA-glucose combinations using RSM

As shown in Fig. 7, the overall obtained results showed that CA and glucose initial concentrations had a significant interactive impact on CA and COD removal, as compared to CMP. The surface plot for CA removal had a clear peak showing that the maximum CA removal could be obtained within the design boundary (Fig. 7a). For the COD removal, the surface convexity was not high enough, suggesting that higher removal efficiency could be observed outside of the designed conditions (Fig. 7b). For the CMP model, little interaction was found for the individual variables, although the critical point of the interaction is shown (Fig. 7c). The optimum combination of CA and glucose was predicted to be 200 mg/L and 2,000 mg/L respectively, which yielded a higher CMP of 160 mL compared to the experimentally determined CMP in this study. Table 3 shows the model fitness results, using analysis of variance (ANOVA) and polynomial regression, for each of the three responses. The obtained second-order models, for each response, were formulated as presented in Eqs. (3)–(5). The R^2 values, for each model, were determined to be 0.92, 0.99 and 0.96 for CA removal, COD removal, and CMP, respectively, and *p*-value less than 0.05 was obtained except for the CA removal model (where *p*-value [0.065] was slightly higher than the significance level of 0.05), suggesting the reasonable fit of model to the experimental data.

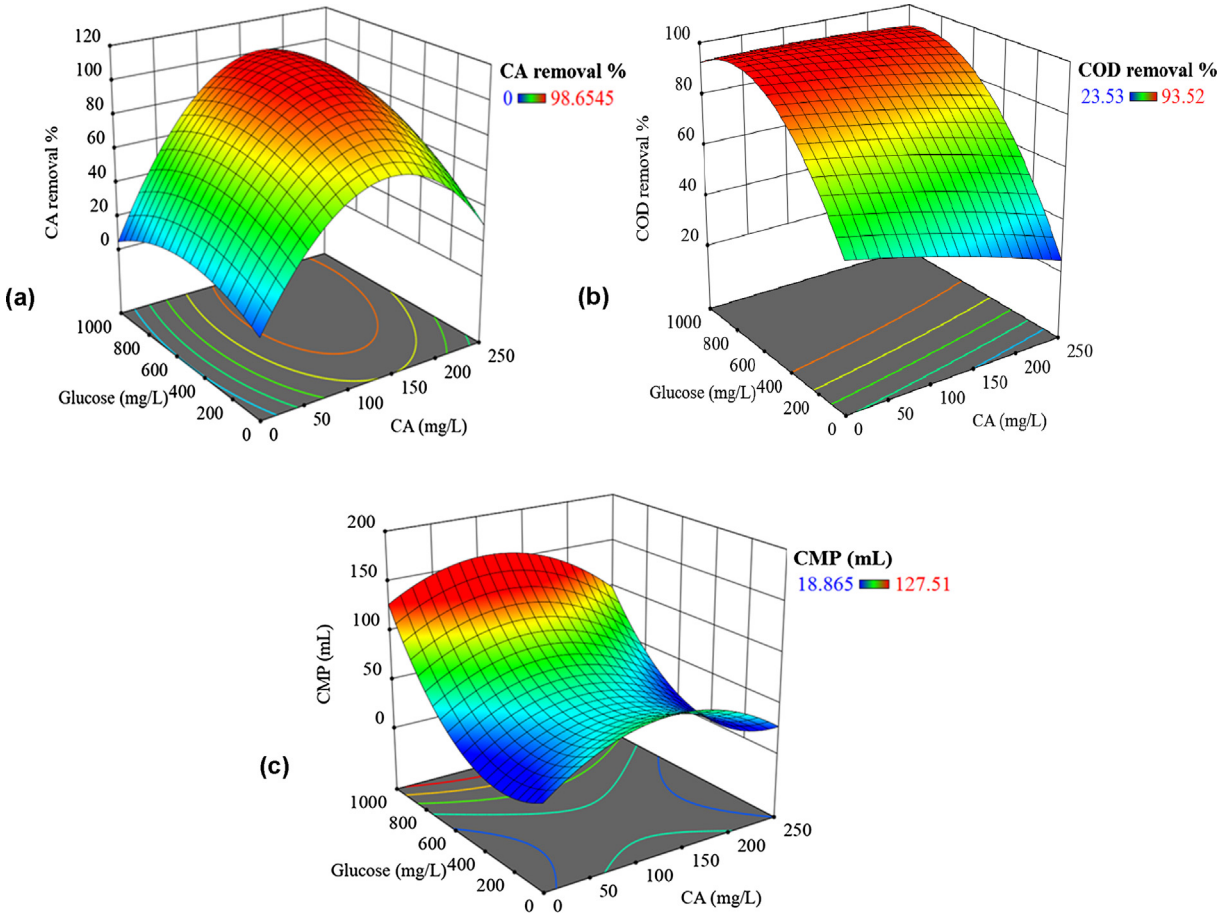

Fig. 7. Response surface plots showing the effect of co-digestion of cyanuric acid (CA) and glucose on the system performance: CA removal (%) (a), COD removal (%) (b), and cumulative methane production (CMP) (c).

Table 3
Model fitness results, using analysis of variance (ANOVA) and polynomial regression, for cyanuric acid (CA) removal (%), COD removal (%), and cumulative methane production (CMP).

Source	Sum of squares	Degree of freedom	Mean square	*F* value	*P* value
CA removal (%) Model	12,700	5	2539	7.4	0.065
A: CA	2679	1	2679	7.8	0.068
B: Glucose	621	1	621	1.8	0.27
AB	626	1	626	1.8	0.27
A^2	691	1	691	2.0	0.25
B^2	60	1	60	0.17	0.71
Residual	1033	3	344		
Total	13,733	8			
R^2 = 0.925, adjusted R^2 = 0.800					
COD removal (%) Model	4680	5	936	111	0.001
A- CA	201	1	201	24	0.016
B- Glucose	3356	1	3356	399	0.000
AB	147	1	147	17	0.025
A^2	0.41	1	0.41	0.049	0.84
B^2	113	1	113	13	0.035
Residual	25	3	8.0		
Total	4705	8			
R^2 = 0.995, adjusted R^2 = 0.986					
CMP Model	10,430	5	2086	15	0.026
A- CA	114	1	114	0.79	0.44
B- Glucose	9108	1	9108	63	0.004
AB	337	1	337	2.4	0.22
A^2	478	1	478	3.3	0.17
B^2	757	1	757	5.3	0.11
Residual	431	3	144		
Total	10,861	8			
R^2 = 0.960, adjusted R^2 = 0.894					

$$Y\,(\text{CA removal},\ \%) = 99 + 24X_1 + 12X_2 + 13X_1X_2 - 53X_1^2 - 16X_2^2 \quad (3)$$

$$Y\,(\text{COD removal},\ \%) = 88 - 6.7X_1 + 27X_2 + 6.1X_1X_2 - 1.3X_1^2 - 22X_2^2 \quad (4)$$

$$Y\,(\text{CMP},\ \text{mL}) = 57 - 5.0X_1 + 45X_2 - 9.2X_1X_2 - 44X_1^2 + 56X_2^2 \quad (5)$$

Conclusions

In this study, continuous and batch-type treatments were conducted to investigate the long-term effect of low CA concentrations on anaerobes, and to improve the CA biodegradability (at high concentrations) via substrate co-digestion. The long-term exposure of mixed culture bacteria to low-strength wastewater (0.6 gCOD/L/d) containing 20 mg/L CA in an anaerobic reactor (i.e., UASR) showed stable performance as well as sludge development (as determined by morphology, XRD, and FTIR analyses). Regarding the microbial community structure, progressed abundance was found, during the long-term incubation, for the genus *Actinobacteria*, which is known to degrade CA. Then, for the high CA concentrations (up to 250 mg/L, as could be existed in some industrial effluents), optimized co-digestion strategy with glucose was suggested. Based on a batch-mode experiment, designed using RSM, the co-digestion of 125 mg/L CA and 750 mg/L glucose achieved the peak CA biodegradation of ~98%. Although higher doses of CA (>125 mg/L) negatively affected the anaerobic process resulting in decrements in methane productivity and COD removal, CA removal of ~77% was recovered when higher glucose (1,000 mg/L) was co-digested with 250 mg/L CA. The progression of CA and urea (i.e., possible CA degradation by-product) degraders and the concurrent generation of NH_4^+-N along with CA degradation profile were consistent with the fact that decomposition of CA and its derivatives occurred in the anaerobic environments examined. Overall, mixed culture anaerobes dealing with low-strength wastewater can efficiently deal with low CA (20 mg/L), whereas the co-digestion with high concentration of readily assimilable substrate, such as glucose, can be an efficient technique when high CA concentrations are existing (up to 250 mg/L).

Compliance with ethics requirements

This article does not describe any studies with human or animal subjects.

Declaration of Competing Interest

The authors declare that they have no known competing financial interests or personal relationships that could have appeared to influence the work reported in this paper.

Acknowledgements

The first author acknowledges Egyptian Ministry of Higher Education (MoHE) and Japan International Cooperation Agency (JICA) for providing all the needed facilities to conduct this research. This study was partially funded by the Japan Society for the Promotion of Science (JSPS) providing Grant-in-Aid for JSPS postdoctoral fellows for research in Japan (18F18061).

References

[1] Seffernick JL, Wackett P. Ancient evolution and recent evolution converge for the biodegradation of cyanuric acid and related triazines 2016;82:1638–45. doi:10.1128/AEM.03594-15.Editor.
[2] Galíndez-Nájera SP, Llamas-Martínez MA, Ruiz-Ordaz N, Juárez-Ramírez C, Mondragón-Parada ME, Ahuatzi-Chacón D, et al. Cyanuric acid biodegradation by a mixed bacterial culture of Agrobacterium tumefaciens and Acinetobacter sp. in a packed bed biofilm reactor. J Ind Microbiol Biotechnol 2009;36:275–84. doi: https://doi.org/10.1007/s10295-008-0496-5.

[3] Yeom S, Mutlu BR, Aksan A, Wackett LP. Bacterial cyanuric acid hydrolase for water treatment. Appl Environ Microbiol 2015;81:6660–8. doi: https://doi.org/10.1128/AEM.02175-15.

[4] An H, Liu J, Li X, Yang Q, Wang D, Xie T, et al. The fate of cyanuric acid in biological wastewater treatment system and its impact on biological nutrient removal. J Environ Manage 2018;206:901–9. doi: https://doi.org/10.1016/j.jenvman.2017.11.073.

[5] Hassan MM, Carr CM. A review of the sustainable methods in imparting shrink resistance to wool fabrics. J Adv Res 2019;18:39–60. doi: https://doi.org/10.1016/j.jare.2019.01.014.

[6] Saldick J. Biological treatment of plant waste streams to remove cyanuric acid, 1974.

[7] Baranda AB, Barranco A, de Marañón IM. Fast atrazine photodegradation in water by pulsed light technology. Water Res 2012;46:669–78. doi: https://doi.org/10.1016/j.watres.2011.11.034.

[8] Azenha MEDG, Burrows HD, Canle LM, Coimbra R, Fernández MI, García MV, et al. Kinetic and mechanistic aspects of the direct photodegradation of atrazine, atraton, ametryn and 2-hydroxyatrazine by 254 nm light in aqueous solution. J Phys Org Chem 2003;16:498–503. doi: https://doi.org/10.1002/poc.624.

[9] Ma L, Chen S, Yuan J, Yang P, Liu Y, Stewart K. International Biodeterioration & Biodegradation Rapid biodegradation of atrazine by Ensifer sp. strain and its degradation genes. Int Biodeterior Biodegradation 2017;116:133–40. doi: https://doi.org/10.1016/j.ibiod.2016.10.022.

[10] Hatakeyama Takashi, Takagi Kazuhiro, Yamazaki Kenichi, Sakakibara Futa, Ito Koji, Takasu Eiichi, Naokawa Takuji, Fujii Kunihiko. Mineralization of melamine and cyanuric acid as sole nitrogen source by newly isolated Arthrobacter spp. using a soil-charcoal perfusion method. World J Microbiol Biotechnol 2015;31(5):785–93. doi: https://doi.org/10.1007/s11274-015-1832-3.

[11] Mukherjee A, Halder S, Datta D, Anupam K, Hazra B, Kanti Mandal M, et al. Free radical induced grafting of acrylonitrile on pre-treated rice straw for enhancing its durability and flame retardancy. J Adv Res 2017;8:73–83. doi: https://doi.org/10.1016/j.jare.2016.12.003.

[12] Velusamy P, Pitchaimuthu S, Rajalakshmi S, Kannan N. Modification of the photocatalytic activity of tio2 by β-cyclodextrin in decoloration of ethyl violet dye. J Adv Res 2014;5:19–25. doi: https://doi.org/10.1016/j.jare.2012.10.001.

[13] Ma Y, Zhang J, Wang Y, Chen Q, Feng Z, Sun T. Concerted catalytic and photocatalytic degradation of organic pollutants over CuS/g-C 3 N 4 catalysts under light and dark conditions. J Adv Res 2019;16:135–43. doi: https://doi.org/10.1016/j.jare.2018.10.003.

[14] Solomon RDJ, Kumar A, Satheeja Santhi V. Atrazine biodegradation efficiency, metabolite detection, and trzD gene expression by enrichment bacterial cultures from agricultural soil. J Zhejiang Univ Sci B 2013;14:1162–72. doi: https://doi.org/10.1631/jzus.B1300001.

[15] Tonelli Fernandes AF, Braz VS, Bauermeister A, Rizzato Paschoal JA, Lopes NP, Stehling EG. Degradation of atrazine by Pseudomonas sp. and Achromobacter sp. isolated from Brazilian agricultural soil. Int Biodeterior Biodegrad 2018;130:17–22. doi: https://doi.org/10.1016/j.ibiod.2018.03.011.

[16] Fernandes AFT, da Silva MBP, Martins VV, Miranda CES, Stehling EG. Isolation and characterization of a Pseudomonas aeruginosa from a virgin Brazilian Amazon region with potential to degrade atrazine. Environ Sci Pollut Res 2014;21:13974–8. doi: https://doi.org/10.1007/s11356-014-3316-7.

[17] El Sebaï T, Devers-Lamrani M, Changey F, Rouard N, Martin-Laurent F. Evidence of atrazine mineralization in a soil from the Nile Delta: Isolation of Arthrobacter sp. TES6, an atrazine-degrading strain. Int Biodeterior Biodegrad 2011;65:1249–55. doi: https://doi.org/10.1016/j.ibiod.2011.05.011.

[18] Benzaquén TB, Isla MA, Alfano OM. Combined chemical oxidation and biological processes for herbicide degradation. J Chem Technol Biotechnol 2016;91:718–25. doi: https://doi.org/10.1007/978-3-662-46635-3_52.

[19] Dodge AG, Preiner CS, Wackett LP. Expanding the cyanuric acid hydrolase protein family to the fungal kingdom 2013;195:5233–41. doi:10.1128/JB.00965-13.

[20] Wazeri A, Elsamadony M, Le Roux S, Peu P, Tawfik A. Potentials of using mixed culture bacteria incorporated with sodium bicarbonate for hydrogen production from water hyacinth. Bioresour Technol 2018;263:365–74. doi: https://doi.org/10.1016/j.biortech.2018.05.021.

[21] Elshahed MS. Microbiological aspects of biofuel production: Current status and future directions. J Adv Res 2010;1:103–11. doi: https://doi.org/10.1016/j.jare.2010.03.001.

[22] Mukherjee D, Bhattacharya P, Jana A, Bhattacharya S, Sarkar S, Ghosh S, et al. Synthesis of ceramic ultrafiltration membrane and application in membrane bioreactor process for pesticide remediation from wastewater. Process Saf Environ Prot 2018;116:22–33. doi: https://doi.org/10.1016/j.psep.2018.01.010.

[23] Cuetos MJ, Martinez EJ, Moreno R, Gonzalez R, Otero M, Gomez X. Enhancing anaerobic digestion of poultry blood using activated carbon Enhancing anaerobic digestion of poultry blood. J Adv Res 2017;8:297–307. doi: https://doi.org/10.1016/j.jare.2016.12.004.

[24] Elreedy A, Fujii M, Koyama M, Nakasaki K, Tawfik A. Enhanced fermentative hydrogen production from industrial wastewater using mixed culture bacteria incorporated with iron, nickel, and zinc-based nanoparticles. Water Res 2019;151:349–61. doi: https://doi.org/10.1016/j.watres.2018.12.043.

[25] Mahmoud M, Elreedy A, Pascal P, Sophie LR, Tawfik A. Hythane (H2 and CH4) production from unsaturated polyester resin wastewater contaminated by 1,4-dioxane and heavy metals via up-flow anaerobic self-separation gases reactor. Energy Convers Manag 2017;152:342–53. doi: https://doi.org/10.1016/j.enconman.2017.09.060.

[26] Meky N, Ibrahim MG, Fujii M, Elreedy A. Integrated dark-photo fermentative hydrogen production from synthetic gelatinaceous wastewater via cost-e ff ective hybrid reactor at ambient temperature 112250. Energy Convers Manag 2020;203. doi: https://doi.org/10.1016/j.enconman.2019.112250.

[27] Yu Y, Park B, Hwang S. Co-digestion of lignocellulosics with glucose using thermophilic acidogens. Biochem Eng J 2004;18:225–9. doi: https://doi.org/10.1016/S1369-703X(03)00127-X.

[28] Wahab MA, Habouzit F, Bernet N, Steyer J-P, Jedidi N, Escudié R. Sequential operation of a hybrid anaerobic reactor using a lignocellulosic biomass as biofilm support. Bioresour Technol 2014;172:150–5. doi: https://doi.org/10.1016/j.biortech.2014.08.127.

[29] Elreedy A, Fujii M, Tawfik A. Psychrophilic hydrogen production from petrochemical wastewater via anaerobic sequencing batch reactor: techno-economic assessment and kinetic modelling. Int J Hydrogen Energy 2019;44:5189–202. doi: https://doi.org/10.1016/j.ijhydene.2018.09.091.

[30] APHA. Standard Methods for the Examination of Water and Wastewater. Washington, DC, USA Am Public Heal Assoc 2012:541. doi:ISBN 9780875532356.

[31] Almomani F, Judd S, Bhosale RR, Shurair M, Aljaml K, Khraisheh M. Intergraded wastewater treatment and carbon bio-fixation from flue gases using Spirulina platensis and mixed algal culture. Process Saf Environ Prot 2019:240–50. doi: https://doi.org/10.1016/j.psep.2019.02.009.

[32] Ali M, Elreedy A, Ibrahim MG, Fujii M, Tawfik A. Hydrogen and methane bio-production and microbial community dynamics in a multi-phase anaerobic reactor treating saline industrial wastewater. Energy Convers Manag 2019;186:1–14. doi: https://doi.org/10.1016/j.enconman.2019.02.060.

[33] Ismail S, Tawfik A. Performance of passive aerated immobilized biomass reactor coupled with Fenton process for treatment of landfill leachate. Int Biodeterior Biodegrad 2016;111:22–30. doi: https://doi.org/10.1016/j.ibiod.2016.04.010.

[34] Takahashi S, Tomita J, Nishioka K, Hisada T, Nishijima M. Development of a prokaryotic universal primer for simultaneous analysis of Bacteria and Archaea using next-generation sequencing e105592. PLoS ONE 2014;9. doi: https://doi.org/10.1371/journal.pone.0105592.

[35] Ismail S, Elsamadony M, Elreedy A, Fujii M, Tawfik A. Physico-chemical and microbial characterization of compartment-wise profiles in an anammox baffled reactor. J Environ Manage 2019;232:875–86. doi: https://doi.org/10.1016/j.jenvman.2018.11.134.

[36] Ali M, Elreedy A, Ibrahim MG, Fujii M, Nakatani K, Tawfik A. Regulating acidogenesis and methanogenesis for the separated bio-generation of hydrogen and methane from saline-to-hypersaline industrial wastewater 109546. J Environ Manage 2019;250. doi: https://doi.org/10.1016/J.JENVMAN.2019.109546.

[37] Zhao J, Li Y, Pan S, Tu Q, Zhu H. Performance of a forward osmotic membrane bioreactor for anaerobic digestion of waste sludge with increasing solid concentration. J Environ Manage 2019;246:239–46. doi: https://doi.org/10.1016/j.jenvman.2019.06.004.

[38] Tang Y, Li M, Xu D, Huang J, Sun J. Application potential of aerobic denitrifiers coupled with a biostimulant for nitrogen removal from urban river sediment. Environ Sci Pollut Res 2018;25:5980–93. doi: https://doi.org/10.1007/s11356-017-0903-4.

[39] Singh P, Suri CR, Cameotra SS. Isolation of a member of Acinetobacter species involved in atrazine degradation 2004;317:697–702. doi:10.1016/j.bbrc.2004.03.112.

[40] Scheff G, Salcher O, Lingens F. Trichococcus flocculiformis gen. nov. sp. nov. A new gram-positive filamentous bacterium isolated from bulking sludge. Appl Microbiol Biotechnol 1984;19:114–9. doi: https://doi.org/10.1007/BF00302451.

[41] Vandewalle JL, Goetz GW, Huse SM, Morrison HG, Sogin ML, Hoffmann RG, et al. Acinetobacter, Aeromonas and Trichococcus populations dominate the microbial community within urban sewer infrastructure. Environ Microbiol 2012;14:2538–52. doi: https://doi.org/10.1111/j.1462-2920.2012.02757.x.

[42] Lü F, Luo C, Shao L, He P. Biochar alleviates combined stress of ammonium and acids by firstly enriching Methanosaeta and then Methanosarcina. Water Res 2016;90:34–43. doi: https://doi.org/10.1016/j.watres.2015.12.029.

[43] Gao M, Zhang L, Florentino AP, Liu Y. Performance of anaerobic treatment of blackwater collected from different toilet flushing systems: Can we achieve both energy recovery and water conservation?. J Hazard Mater 2019;365:44–52. doi: https://doi.org/10.1016/j.jhazmat.2018.10.055.

[44] Aida AA, Hatamoto M, Yamamoto M, Ono S, Nakamura A, Takahashi M, et al. Molecular characterization of anaerobic sulfur-oxidizing microbial communities in up-flow anaerobic sludge blanket reactor treating municipal sewage. J Biosci Bioeng 2014;118:540–5. doi: https://doi.org/10.1016/j.jbiosc.2014.04.011.

[45] Vigil de la Villa R, Frías M, Sánchez de Rojas MI, Vegas I, García R. Mineralogical and morphological changes of calcined paper sludge at different temperatures and retention in furnace. Appl Clay Sci 2007;36:279–86. doi: https://doi.org/10.1016/j.clay.2006.10.001.

[46] Belmokhtar N, El Ayadi H, Ammari M, Ben Allal L. Effect of structural and textural properties of a ceramic industrial sludge and kaolin on the hardened geopolymer properties. Appl Clay Sci 2018;162:1–9. doi: https://doi.org/10.1016/j.clay.2018.05.029.

[47] Nyobe JB. Application of normative calculations in quantitative comparative mineralogical studies of bauxite. Ore Geol Rev 1991;6:45–50. doi: https://doi.org/10.1016/0169-1368(91)90031-2.

[48] Zhao X, Ma J, Ma H, Gao D, Sun Y, Guo C. Removal of polyacrylate in aqueous solution by activated sludge: Characteristics and mechanisms. J Clean Prod 2018;178:59–66. doi: https://doi.org/10.1016/j.jclepro.2017.12.215.
[49] Li X, Dai X, Takahashi J, Li N, Jin J, Dai L, et al. New insight into chemical changes of dissolved organic matter during anaerobic digestion of dewatered sewage sludge using EEM-PARAFAC and two-dimensional FTIR correlation spectroscopy. Bioresour Technol 2014;159:412–20. doi: https://doi.org/10.1016/j.biortech.2014.02.085.
[50] Chan WP, Wang JY. Formation of synthetic sludge as a representative tool for thermochemical conversion modelling and performance analysis of sewage sludge – Based on a TG-FTIR study. J Anal Appl Pyrolysis 2018;133:97–106. doi: https://doi.org/10.1016/j.jaap.2018.04.015.
[51] Farhat A, Asses N, Ennouri H, Hamdi M, Bouallagui H. Combined effects of thermal pretreatment and increasing organic loading by co-substrate addition for enhancing municipal sewage sludge anaerobic digestion and energy production. Process Saf Environ Prot 2018;119:14–22. doi: https://doi.org/10.1016/j.psep.2018.07.013.
[52] De Oliveira Silva J, Filho GR, Da Silva Meireles C, Ribeiro SD, Vieira JG, Da Silva CV, et al. Thermal analysis and FTIR studies of sewage sludge produced in treatment plants. The case of sludge in the city of Uberlândia-MG. Brazil. Thermochim Acta 2012;528:72–5. doi: https://doi.org/10.1016/j.tca.2011.11.010.
[53] Shiomi N, Yamaguchi Y, Nakai H, Fujita T, Katsuda T, Katoh S. Degradation of cyanuric acid in soil by Pseudomonas sp. NRRL B-12227 using bioremediation with self-immobilization system. J Biosci Bioeng 2006;102:206–9. doi: https://doi.org/10.1263/jbb.102.206.
[54] Cook AM, Beilstein P, Grossenbacher H, Hotter R. Ring cleavage and degradative pathway of cyanuric acid in bacteria 1985;231:25–30.
[55] Desitti C, Beliavski M, Tarre S, Green M. Stability of a mixed microbial population in a biological reactor during long term atrazine degradation under carbon limiting conditions. Int Biodeterior Biodegrad 2017;123:311–9. doi: https://doi.org/10.1016/j.ibiod.2017.07.007.
[56] Chan CY, Tao S, Dawson R, Wong PK. Treatment of atrazine by integrating photocatalytic and biological processes. Environ Pollut 2004;131:45–54. doi: https://doi.org/10.1016/j.envpol.2004.02.022.
[57] Radosevich M, Traina SJ, Tuovinen OH. Degradation of binary and ternary mixtures of s-triazines by a soil bacterial isolate. J Environ Sci Heal Part B 1995;30:457–71. doi: https://doi.org/10.1080/03601239509372947.
[58] Ernst C, Rehm HJ. Development of a continuous system for the degradation of a cyanuric acid by adsorbed Pseudomonas sp. NRRL B-12228. Appl Microbiol Biotechnol 1995;43:150–5. doi: https://doi.org/10.1007/BF00170637.
[59] Bhardwaj P, Sharma A, Sagarkar S, Kapley A. Mapping atrazine and phenol degradation genes in Pseudomonas sp. EGD-AKN5. Biochem Eng J 2015. doi: https://doi.org/10.1016/j.bej.2015.02.029.